Structural Engineering and Mechanics, *Vol. 64, No. 3 (2017) 353-360*
DOI: https://doi.org/10.12989/sem.2017.64.3.353

BB-BC optimization algorithm for structural damage detection using measured acceleration responses

J.L. Huang and Z.R. Lu*

Department of Applied Mechanics, Sun Yat-sen University, Guangzhou, Guangdong Province, 510006, P.R. China

(Received July 13, 2016, Revised August 9, 2017, Accepted August 18, 2017)

Abstract. This study presents the Big Bang and Big Crunch (BB-BC) optimization algorithm for detection of structure damage in large severity. Local damage is represented by a perturbation in the elemental stiffness parameter of the structural finite element model. A nonlinear objective function is established by minimizing the discrepancies between the measured and calculated acceleration responses (AR) of the structure. The BB-BC algorithm is utilized to solve the objective function, which can localize the damage position and obtain the severity of the damage efficiently. Numerical simulations have been conducted to identify both single and multiple structural damages for beam, plate and European Space Agency Structures. The present approach gives accurate identification results with artificial measurement noise.

Keywords: damage detection; time domain; BB-BC algorithm; optimization

1. Introduction

Existing damages in vital structures present serious threats to safety of life and property. Various factors can be blamed for the degradation of structural strength or stiffness, such as natural disasters (e.g. storms), fatigue, corrosion, etc. Therefore, structural health monitoring (SHM) techniques, which can help to localize and quantify the damage, are of great importance. Generally, the damage detection technique contains vibration signals analysis, or other physical property analysis, and optimization algorithm to identify damages in structures in an efficient way. Modal parameters have been used extensively in the SHM process and most of the existing damage identification methods are mainly based on the changes of frequencies or the frequency response function (FRF): Baghmisheh (2012) found the optimal crack location and depth in a cantilever beam by minimizing the cost function which is based on the difference of the first four measured and calculated natural frequencies and Yang (2014) presented a damage identification technique based on optimization processes and embedded sensitivity analysis that requires only measured or calculated frequency response functions to obtain the sensitivity of system responses to each component parameter; Ratcliffe (1997) used a modified Laplacian operator on mode shape data to detect the damage in structures. Mehrjoo (2013) suggested that the combination fitness function of natural frequencies with mode shapes can represent the solution with better results. Yang (2011) and Sung *et al*.(2014), these researchers proposed damage identification methods based on Structural flexibility.

On the other hand, dynamic responses of the structures have been applied to damage detection as the structural damage identification in the time domain attracts the interest of many researchers. Koh *et al*. (2000) and Mahumder and Majumder (2003) both used a time domain approach for damage detection in beam structures and large structural systems, respectively. Lu and Law (2007) applied dynamic response sensitivity features to damage detection; Bu *et al*. (2006) used response sensitivity to surveil the vehicle condition on continuous bridges. Lu and Liu (2011) proposed an identification method for structural damages in both bridge deck and vehicular parameters using measured dynamic responses.Li *et al*.(2016) and Fu *et al*.(2016) suggested that response sensitivity analysis can be used to quantify the extent of internal damage. Cattarius and Inman (1997) used time histories of the vibration response of the structure for identifying the presence of damage.

From a mathematical point of view, the damage identification problem can be transformed into an optimization problem. In the past few decades, various optimization algorithms have been proposed for structural damage identification. For instance, Genetic Algorithm (GA), Simulated Annealing (SA), Particle Swarm Optimization (PSO), Ant Colony Optimization (ACO), artificial bee conoly (ABC) algorithm, Fruit Fly Optimization (FOA), etc. have been used in the damage identification process. After formulating a fitness function by proposed studies on physical nature, the optimization algorithms are here to speed up the convergence process, achieving a satisfactory result ultimately. Mohan and Maiti (2013) used Frequency Response Function (FRF) with the help of the Particle Swarm Optimization (PSO) technique proposed by Kennedy and Eberhart (1997), for structural damage detection and quantification. Abdelali *et al*. (2014) used the PSO to access the location of impact force. Xu *et al*. (2015) applied the chaotic artificial bee colony algorithm to damage detection. Taghi *et al*. (2008) made use of

*Corresponding author, Professor
E-mail: lvzhr@mail.sysu.edu.cn

ISSN: 1225-4568 (Print), 1598-6217 (Online)

genetic algorithms (GA) and a model of damaged (cracked) structure to detect the crack in beam-like structures. In this process, the natural frequencies are obtained through numerical methods. Kwon *et al*. (2008) used successive zooming genetic algorithm to detect the damage in continuum structures. Miguel Fleck Fadel Miguel (2013) presented a hybrid stochastic/deterministic optimization algorithm to solve the target optimization problem of vibration-based damage detection containing a fitness function that consisted of natural frequency and mode shapes. Yi *et al*. (2015) tried to apply the collaborative-climb monkey algorithm to the health monitoring of high-rise structures. Li and Lu (2015) suggested that the Multi-Swarm Fruit Fly optimization algorithm can be used in structural damage identification. The Big Bang-Big Crunch was first proposed by Erol and Eksin (2006), and their study showed that the main drawback of the classical GA in the term of convergence speed might be overcome by the new BB-BC method. Tab and Afshri (2013) proposed the BB-BC algorithm as optimization method in damage detection with an objective function based on natural frequencies and mode shapes in frequency domain.

In practice, natural frequencies, especially the higher ones, can be measured accurately, but it is difficult to obtain the accurate mode shapes. In this study, we try to address the problem in time domain and directly make use of the acceleration responses of the structures. In the identification, an objective function is established by minimizing the differences of measured acceleration responses, which are usually the responses of damaged structures, and computed ones (initially, the computed responses are those of the healthy structures). The BB-BC algorithm is then used to solve the objective function to obtain the optimal solutions the locations and extents of the structural damages. Three numerical examples, namely a simply supported beam, a cantilever plate and the European Space Agency Structure, are studied to show the accuracy and robustness of the proposed method. The artificial measurement noise and both single and multiple damage cases are considered in each numerical example. Identification results in the numerical simulation section suggested that all the accuracy of estimation of damages can be obtained within a small range of error, even with 10% noise from the present damage identification method.

2. Theory

2.1 Forward analysis

The equation of motion for a general FE model of a linear elastic health structural dynamic system, which serves as the baseline for a damage detection problem, can be described as

$$M\ddot{u} + C\ddot{u} + Ku = F(t) \tag{1}$$

where *K* and *M* are the global stiffness and mass matrices of the health structural model, respectively; *C* is the Rayleigh damping matrix, which can be expressed as $C = a_1 M + a_2 K$ in this study, u, $\dot{u}$and $\ddot{u}$are displacement, velocity and acceleration responses of the healthy structure, respectively. $F(t)$ is the vector of external excitation force. In this study, the well-known Newmark direct integration method is used to obtain the dynamic responses of the structure .

In the context of damage identification, it generally assumes that there will be a decrease in the stiffness parameters while the mass property remains unchanged. For the above reason, the damage parameter $\boldsymbol{\alpha}$ is introduced to describe the change of stiffness, which can be illustrated as

$$K_d = \sum_{i=1}^{nel} \alpha_i \, k_i \tag{2}$$

where K_d is the global stiffness matrix of the damaged structure; k_i represents the i^{th} elemental stiffness matrix, α_i is the damage parameter, indicating the damage severity of the i^{th} element and nel is the number of elements. The element stays intact while $\alpha_i = 1$ and becomes completely destructive when $\alpha_i = 0$.

The corresponding elastic equation of damaged structures can be expressed as follows

$$M\ddot{u}_d + C_d\ddot{u}_d + K_d u_d = F(t) \tag{3}$$

where $\ddot{u}_d$, $\dot{u}_d$ and u_d are the acceleration, velocity and displacement responses of damaged structures, respectively.

2.2 The objective function for inverse problem

In the identification, the damage parameters can be obtained by formulating an optimization problem in which the error of dynamic response value between the computed and measurement is minimized. The objective function can be expressed as the residual between the measured and calculated acceleration responses

$$Acc(\boldsymbol{\alpha}) = \frac{1}{2}\sum_{j=1}^{\beta}\sum_{i=1}^{\mu t}(\ddot{u}_{mij} - \ddot{u}_{cij})W(\ddot{u}_{mij} - \ddot{u}_{cij}) \tag{4}$$

where $\ddot{u}_{mij}$ and $\ddot{u}_{cij}$ are the vectors of measured and calculated acceleration response respectively, W represents the weighting matrix.

The damage parameters can be obtained by minimize the objective function, shown as below

$$Minimize\colon\ Acc(\boldsymbol{\alpha}),\ \ Subject\ to\ \ 0 < \boldsymbol{\alpha} < 1 \tag{5}$$

2.3 Effect of artificial measurement noise

The numerical simulations will study the effect of the artificial measurement noise existing in the damage detection process to consider the errors in the measurements. White noise contained in the calculated acceleration responses is used to simulate the noise data with

$$\hat{\ddot{u}} = \ddot{u} + E_p \cdot N_{noise} \cdot \sigma(\ddot{u}) \tag{6}$$

where E_p is the percentage noise level (e.g. 0.1 relates to a 10% noise level), N_{noise} is a standard normal distribution with zero mean and unit standard variance. In this paper $\sigma(\ddot{u})$ is the standard deviation of the calculated

acceleration response.

3. Brief introduction to BB-BC optimization algorithm

In BB-BC algorithm, randomness represents the energy distribution irregularly in the initial universe, while the gravitational attraction between each individual forces the random mass items with energy to converge to an optimum point. Since energy dissipation creates disorder from ordered particles, we will use randomness as a transformation from a converged solution (order) to the birth of totally new candidates (disorder or chaos). The complete BB-BC algorithm consists of three phases; the Big Bang Phase, Calculation of the fitness function value, the Big Crunch Phase. These will be specifically described as follows.

3.1 The big band phase

Initially, the process starts from the Big Bang Phase, in which each random mass particles with random energy can be seen as a solution to the problem. An n-dimension search space *X*, containing *i* candidates with limitations in every dimension, has been set in this phase

$$\tilde{X} = \{\boldsymbol{X_1}, \boldsymbol{X_2}, \boldsymbol{X_3}, \dots, \boldsymbol{X_i}\} \quad i = 1,2,3, \dots$$
$$\boldsymbol{X_i} = [x_1, x_2, x_3, \dots, x_n] \quad n = 1,2,3, \dots$$

where $\boldsymbol{X_i}$ is the i^{th} candidate in the search space; and $x_k (1 \le k \le n)$ is the k^{th} eleme1nt in a solution candidate, which should be set as a random number within the search space.

3.2 Calculation of the fitness function value

This algorithm simulates the evolution of the primal universe, the inverse of the fitness value of every candidate can be seen as gravitational attraction. After producing the candidates, the fitness function value of each candidate can be obtained through Eq. (5). In this process, the best local result can be obtained according to the smallest fitness value

$$Acc(\boldsymbol{X}^{lbest}) = f^{best} \tag{7}$$

where $\boldsymbol{X}^{lbest}$ and f^{best} denote the best candidates and the smallest fitness function value in the local search, respectively.

3.3 The big crunch phase

In this phase, the BB-BC algorithm is aimed to force all the randomness dissipation converge to a optimum point on the basis of the inverse of the fitness function value. This process may generate a new larger mass particle named center mass, shown as below

$$\boldsymbol{X^C} = \frac{\sum_{i=1}^{n} \frac{1}{f^i} \cdot \boldsymbol{X}_i}{\sum_{i=1}^{n} \frac{1}{f^i}} \tag{8}$$

where the $\boldsymbol{X^C}$ denotes a new center mass in the Big Crunch Phase and f^i indicates the fitness function value in the i^{th} iteration;

The new candidates will be generated beside center mass and is given by

$$\boldsymbol{X}^{new} = w^g \boldsymbol{X^C} + (1 - w^g) \cdot \boldsymbol{X}^{lbest(k)} + \frac{l \cdot \boldsymbol{r}}{k} \tag{9}$$

where the $\boldsymbol{X}^{new}$ represents new candidates, w^g manages the balance of the local and global search and $\boldsymbol{X}^{lbest(k)}$ is the best local solution in the k^{th} iteration. l is the limitation parameter to control the n-dimension confine of the search space, while $\boldsymbol{r}$ is a normal random vector with the same dimension as the last generation of candidates; k is the iteration number, which is used to reduce the search space for each iteration for an accurate optimal result.

In this paper the BB-BC algorithm parameters are set as follows, after trials to suit the problem: the maximum number of generations will vary for different cases, and will be mentioned under the numerical simulations section; Population size remains 30 throughout, $w^g = 0.8$ for beam and plate structures and $w^g = 0.5$ for European Space Agency Structure initially and is increased linearly with time until $w^g = 1$.

4. Numerical simulation

In this section, three different structures are studied as examples to evaluate the effectiveness and robustness of the proposed method. 10% artificial measurement noise is contained in every damage identification case. It may be observed that the results with noise in some specific elements will be even better than the results without noise. This is because the errors that have been considered in this paper are distributed in all elements, and the total accumulated errors in a case with noise will obviously be larger than that without noise. This can be easily indicated by the detection result figure: at the assumed intact elements, situations with noise will have prediction results much larger than 0. In addition, it may be noticed that the maximum number of iterations in trial cases are different (e.g., maximum generation number in case 3 and case 4 are 1400 and 2000, respectively.) This value is increased due to the increase of complexity of structures. With more iterations, the algorithm is able to converge and deliver more reasonable results, rather than termination before convergence. Detection results of both single and multiple damage situations are displayed with the comparison of the difference of their dynamic response vectors.

4.1 A simply supported beam

A simply supported beam is studied as the first numerical example, as shown in Fig. 1. The physical parameters of the structure are as follows: mass density $\rho = 2.8 \times 10^3$ kg/m^3, Young's modulus $E = 34$ Gpa, total length $L = 30$ m , width $b = 0.5$ m and height $h = 1.0$ m .The FE model of the beam consists of 10 Euler-Bernoulli beam elements with two DOFs at each node. The total number of DOFs is 22.

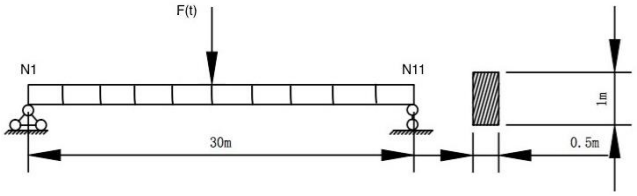

Fig. 1 Finite element model of a simply supported beam structure

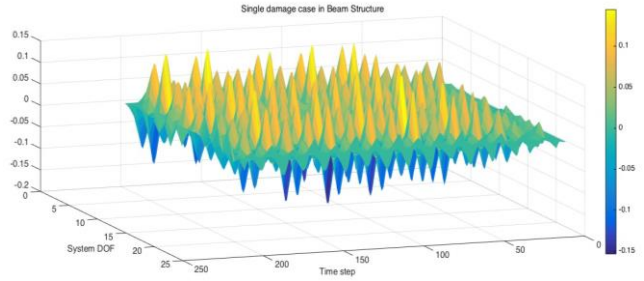

Fig. 2 The difference of acceleration response (AR) between single damaged and healthy beam structures

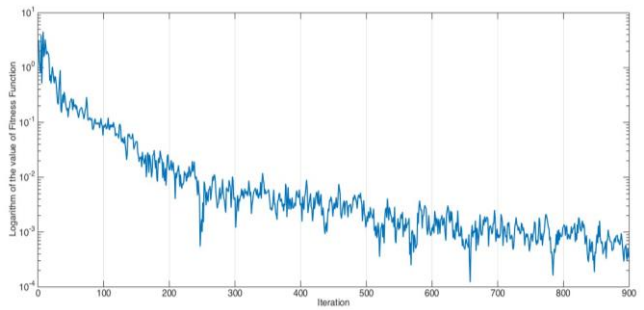

Fig. 3 The value of fitness function versus the number of generation for damage case 1

In the process of computing the dynamic response, the single time step is 0.005s and the lasting time is 1s throughout this study. The Rayleigh damping model is used as both damping parameters mentioned in Eq. (1) are 0.01. To obtain the dynamic response, a sinusoidal excitation force is applied 15 m away from the left end of this beam structure, which is shown as

$$F(t) = 10000 \times \sin(19\pi t) \quad N \tag{10}$$

Case 1: Single damage in beam structure

In this damage case, the damage parameter is $\alpha_5 = 0.3$, as it is assumed that the 5^{th} element has 30% reduction of EI. The error of acceleration response of each DOF between the damaged and intact structure is shown in Fig. 2. This difference can be used in the fitness function to find not only the location but also the extent of damage to the structure, as mentioned in the **Theory** section. Fig. 3 presents the iteration process of fitness function, which can indicate that the identified damage parameters converged to the desired values after 500 iterations. The final detection results, which can tell the accuracy and robustness of the proposed method, are shown in Fig. 4 and Table. 1: with 10% artificial noise, the corresponding identification error

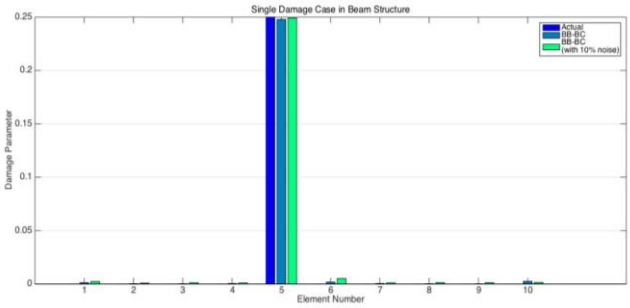

Fig. 4 Detection results for damage case 1

Table 1 Results for single damage identification of the beam structure

Element NO.5			
Scenarios	Noise	Identified (%)	Error (%)
Actual	Nil	25.00	0.00
1	Nil	24.78	0.88
2	10%	24.92	0.32

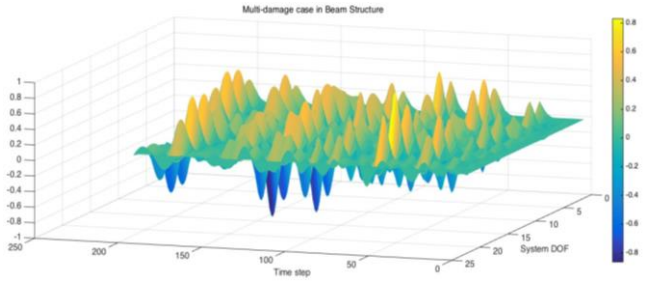

Fig. 5 The difference of AR between multiple damaged and healthy beam structures

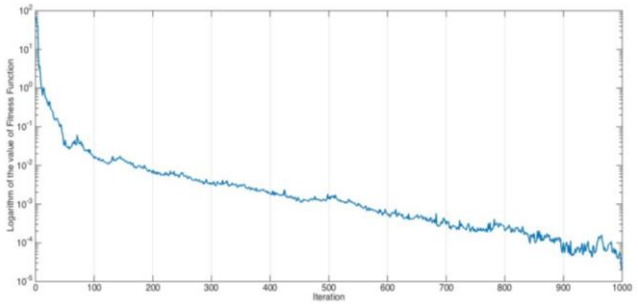

Fig. 6 The value of fitness function versus the number of generations for damage case 2

is 3.2% In this case, it may be seen that the result with noise in element No. 5 is better than that without noise, however, since the errors are distributed and accumulate in all elements, results with noise in element No. 1 and No. 6 are much worse than those without noise, which should be 0 for those intact elements.

Case 2: Multi-damage in beam structure

In the multi-damage case, 50%, 20% and 10% damage has been considered in elements 3, 5 and 9 respectively. Fig. 5 shows the difference of acceleration response between multiple damaged structure and the healthy beam

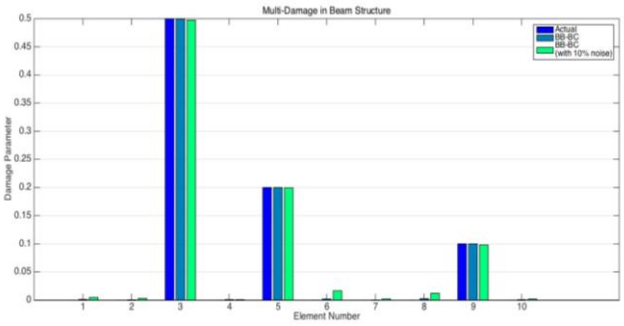

Fig. 7 Detection results for damage case 2

Table 2 Results for multi-damage identification of the beam structure

Scenarios	Noise	Element No.3		Element No.5		Element No.9	
		Identified (%)	Error (%)	Identified (%)	Error (%)	Identified (%)	Error (%)
Actual	Nil	50.00	0.00	20.00	0.00	10.00	0.00
1	Nil	49.95	0.10	20.01	0.05	9.70	3.00
2	10%	49.73	0.54	19.97	0.15	8.01	19.90

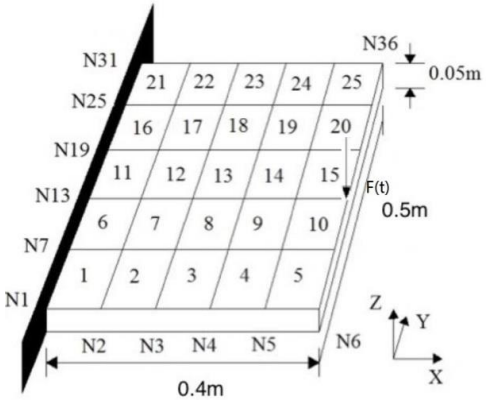

Fig. 8 Finite element model of the cantilever plate structure

structures, shows the unique characteristics of the multi-damage structure studied in this case. The maximum generation of 1000 is used in this case, the fitness function value converges to 10^{-4} finally, which can be seen in Fig. 6.

4.2 Cantilevered plate

A cantilevered plate is further investigated to evaluate the proposed method. The plate has a fixed end at the left with the length=0.4 m, width=0.5 m and thickness=0.05 m shown in Fig. 8. The physical material properties of the structure are: density $\rho = 2800\ \mathrm{kg/m^3}$, Young's modulus $E = 25\ \mathrm{Gpa}$, and Poisson ratio $\mu = 0.3$ .The plate is divided into 25 4-node Reissner-Mindlin plate elements. As the left end is completely fixed, the total DOFs is 108. It is assumed that a sinusoidal excitation force is applied at the the 18^{th} node in the z direction, which is shown as Eq. (11) and indicated in Fig. 8. To obtain the dynamic response, the single time step is set as 0.005s, lasting 1s, while the Rayleigh parameters are equal to 0.01. Six acceleration measurement points: 17^{th}, 23^{rd}, 41^{st}, 48^{th}, 58^{th}, and 67^{th} are used to identify the damage in the plate.

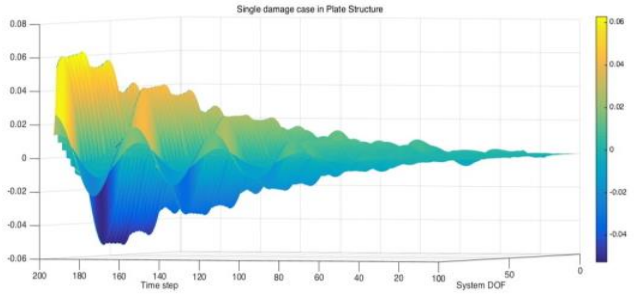

Fig. 9 The difference of AR between single damaged and healthy plate structures

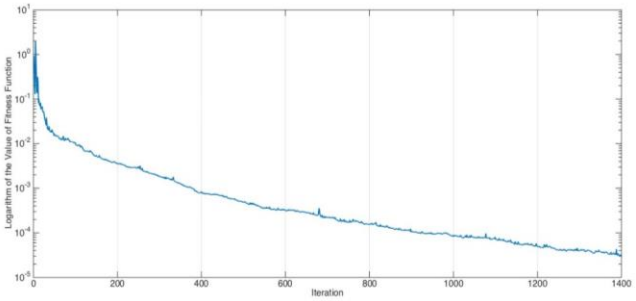

Fig. 10 The value of fitness function versus the number of generation for damage case 3

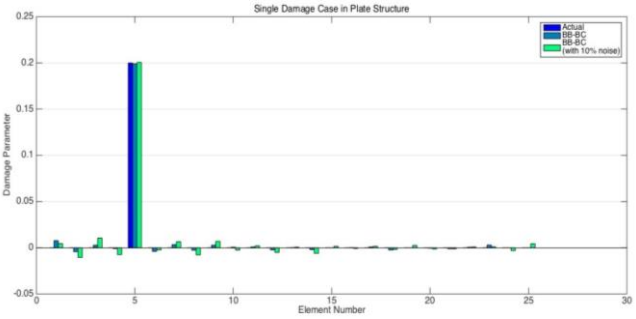

Fig. 11 Detection results for damage case 3

Table 3 Results for single damage identification of the plate structure

Element NO.5			
Scenarios	Noise	Identified (%)	Error (%)
Actual	Nil	20.00	0.00
1	Nil	19.90	0.50
2	10%	20.06	0.30

$$F(t) = 20 \times \sin(10\pi t) \quad N \tag{11}$$

Case 3: Single damage in plate structure

This case assumes that the 5^{th}element has 20% reduction in EI, therefore the damage parameter $\alpha_5 = 0.8$ .With the maximum generation of 1400, and with a fitness value under 10^{-4}, results are shown in Fig. 11, while the damage identification results with small errors are shown in Table 3 and Fig. 11. Fig. 10 is the error value of AR. The

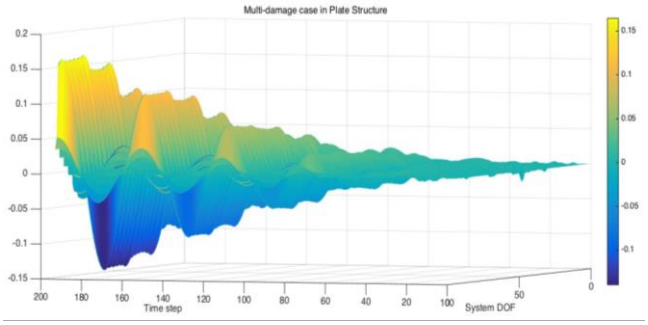

Fig. 12 The difference of AR between multiple damaged and health plate structures

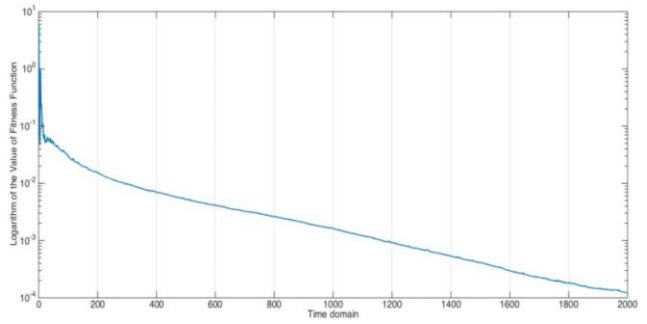

Fig. 13 The value of fitness function versus the number of generations for damage case 4

Table 4 Results for multi-damage identification of the plate structure

Scenarios	Noise	Element No.4		Element No.11		Element No.14		Element No.23	
		Identified (%)	Error (%)	Identified (%)	Error (%)	Identified (%)	Error (%)	Identified (%)	Error (%)
Actual	Nil	20.00	0.00	30.00	0.00	30.00	0.00	10.00	0.00
1	Nil	20.23	1.15	30.18	0.60	29.35	2.16	9.70	3.00
2	10%	20.97	4.85	20.91	0.30	30.20	0.76	8.01	19.9

BB-BC algorithm can identify both the location and severity of the damage to the structure by the tiny difference from -0.06 to 0.08, and achieve pre-assumed accuracy with 3.0% error under 10% artificial noise. This shows the outstanding sensitivity of the proposed method.

Case 4: Multi-damage in plate structure

In the multi-damage case of plate structure, 4 elements with desired reduction of EI as following: 20% (Element No. 4), 30% (Element No. 11), 30% (Element No. 14), 10% (Element No. 23) are introduced to testify to the accuracy of the proposed method. The maximum generation in this case is 2000, and Fig. 12 shows the error of AR, while damage identification results are described in Table 4 and Fig. 14.

In Fig. 12, we can see that the error of AR increase by the time and it changed noticeably after time=140, indicating the vibration property of the cantilevered structure differed from the beam and European Space Agency Structure. The values of AR in the beam structure and European Space Agency Structure, shown in Fig. 5 and Fig. 19, shows that the perturbation of acceleration occurs at the beginning of the time histories.

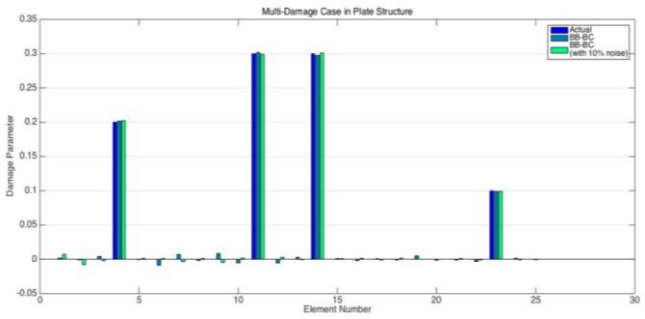

Fig. 14 Detection results for damage case 4

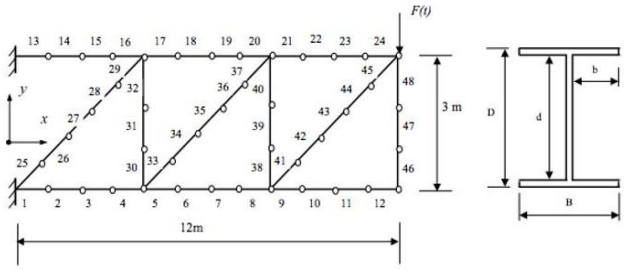

B	D	b	d
0.5	0.8	0.235	0.75

Fig. 15 Finite element model of the European Space Agency Structure

4.3 The European Space Agency Structure

The European Space Agency Structure (ESAS) is studied as another numerical example to validate the effectiveness of the proposed method. The finite element model (FEM) of the structure ESAS is shown in Fig. 15. The structure is modeled by 48 European Space Agency Structure elements and 44 nodes with three DOFs at each node for the translation and rotational deformations. Each European Space Agency Structure element is constructed by integrating a Euler-Bernoulli beam element with a rod element. The modulus of elasticity of material is assumed to be $E = 7.5 \times 10^{10}\ \mathrm{N/m^2}$ and the mass density is $\rho = 2800\ \mathrm{kg/m^3}$. The total number of DOFs specified in the finite element model is 132. The first eight natural frequencies of the undamaged ESAS structure are 16.86, 63.13, 80.05, 131.34, 173.33, 196.23, 201.73 and 214.42Hz. Rayleigh damping model is used for constructing the damping matrix and the modal damping ratios of the first two modes are taken as 0.01 and 0.02 respectively. The single time step is 0.005 and the total lasting time is 1s, the sinusoidal excitation force is set at the 77^{th} DOF shown as below

$$F(t) = -5000 \times \sin(16\pi t) \quad N \tag{12}$$

Case 5: Single damage in European Space Agency Structure

In this damage case, element No. 17 has a desired 30% reduction in EI while 4000 is given as the maximum

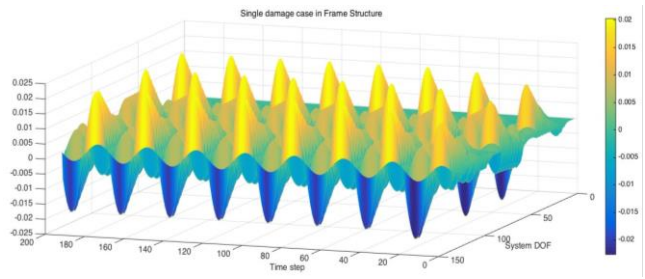

Fig. 16 The difference of AR between single damaged and healthy European Space Agency Structures

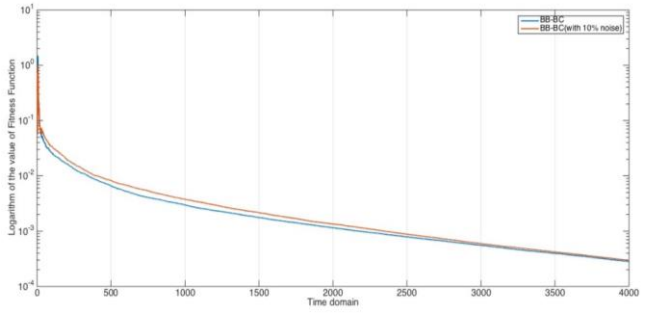

Fig. 17 The value of fitness function versus the number of generation for damage case 5

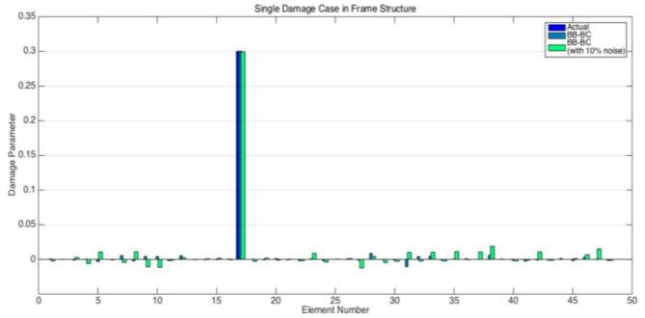

Fig. 18 Detection results for damage case 5

Table 5 Result for single damage identification of the European Space Agency Structure

Element NO. 17			
Scenarios	Noise	Identified (%)	Error (%)
Actual	Nil	30.00	0.00
1	Nil	30.03	1.00
2	10%	29.94	2.00

generation for the proposed method to identify the damage location and severity. Fig. 16 shows the acceleration between the damaged and intact structures, and the obvious difference exists throughout the process. The fitness value obtained with artificial noise and without it are both shown in Fig. 17. The algorithm with noise can achieve almost the same accuracy as the one without noise, which confirms the robustness of the proposed algorithm. The detection results are shown in Fig. 18 and Table 5.

Case 6: Multi-damage in European Space Agency Structure

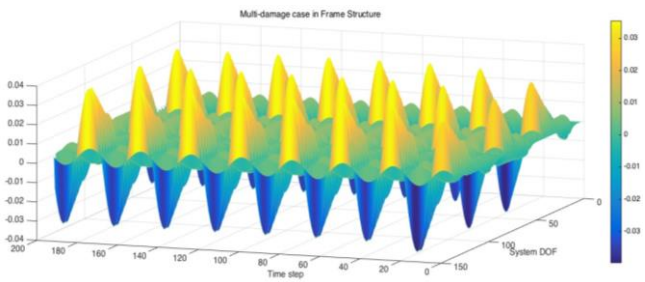

Fig. 19 The difference of AR between multiple damaged and healthy European Space Agency Structures

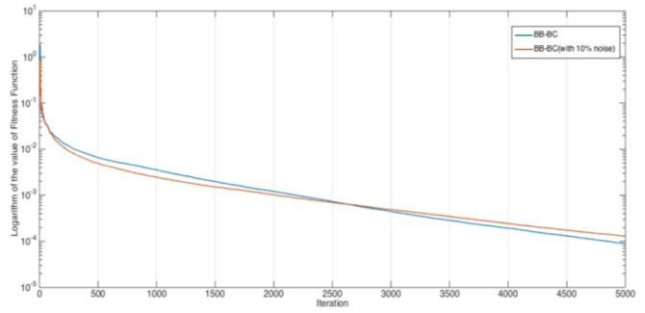

Fig. 20 The value of fitness function versus the number of generations for damage case 6

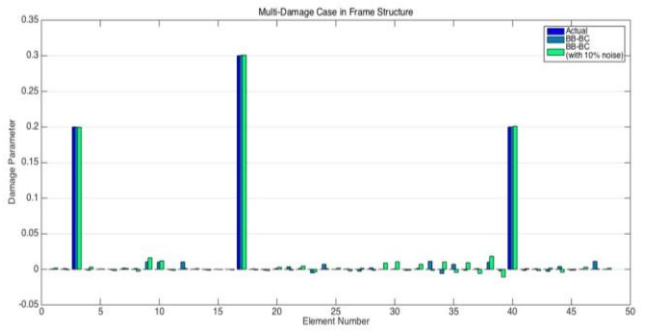

Fig. 21 Detection results for damage case 6

Table 6 Results for multi-damage identification of the European Space Agency Structure

Scenarios	Noise	Element No.3		Element No.17		Element No.40	
		Identified (%)	Error (%)	Identified (%)	Error (%)	Identified (%)	Error (%)
Actual	Nil	20.00	0.00	30.00	0.00	20.00	0.00
1	Nil	19.96	0.20	30.06	0.20	20.81	4.05
2	10%	19.96	0.20	30.10	0.33	22.21	11.05

In these damage cases, it assumes that elements 3, 17 and 40 have 20%, 30% and 20% damage reduction respectively, while 5000 is the maximum generation. Though testing may be a little time-consuming, as the number of elements increased, the sensitivity of fitness on the BB-BC algorithm may have been affected, which may make the convergence process more difficult to achieve or compromise the accuracy. In this study, although the elements in the European Space Agency Structure reach as high as 48 with 132 DOFs, a good result can still be obtained with an error rate under/around 10^{-4} as shown in

Fig. 20. The detection results are shown in Fig. 21 and Table. 6

5. Conclusions

A robust methodology is presented in this study to identify and quantify damages in the structures applying AR as input response in the BB-BC algorithm. The proposed method has been tested on a simply supported beam, a cantilevered plate and the European Space Agency Structure with different damage cases. Both single and multiple damages can be detected with satisfactory accuracy. The detection processes affected by the artificial noise measurements also show the desired results. Though the proposed method can prove convincing detection results, a further study on the improvement of efficiency can be conducted in the future.

Acknowledgments

This work was supported by the National Natural Science Foundation of China under Grants (11572356), Guangdong Province Natural Science Foundation (2015A030313126), and the Guangdong Province Science and Technology Program (2016A020223006). Such financial aids are gratefully acknowledged.

References

El-Bakari, A., Khamlichi, A., Jacquelin, E. and Dkiouak, R. (2014), "Assessing impact force localization by using a particle swarm", *J. Sound Vib.*, **333**, 1554-1561

Baghmisheh, M.V., Peimani, M., Sadeghi, M.H., Ettefagh, M.M. and Tabrizi, A.F. (2012), "A hybrid particle swarm-Nelder-Mead optimization method for crack detection in cantilever beams", *Appl. Soft Comput.*, **12**, 2217-2226

Cattarius, J. and Inman, D. J. (1997), "Time domain anaylysis for damage detection in smart structures", *Mech. Syst. Signal Pr.*, **11**(3), 409-423

Erol, K.O. and Eksin, I. (2006), "A new optimization method: Big Bang-Big Crunch", *Adv. Eng.Softw.*, **37**, 106-111

Fu, Y.Z., Liu, J.K., Wei, Z.T. and Lu, Z.R. (2016) "A two-step approach for damage identification in plates", *J. Vib. Control*, **22**(13), 3018-3031

Kennedy, J. and Eberhart, R. (1995), "Particle swarm optimization", *IEEE International Conference on Neural Networks*, 1942-1948

Koh, C.G., Hong, B. and Liaw, C.Y. (2000), "Parameter identification of large structural systems in time domain", *J. Struct. Eng.*, ASCE, **126**(8), 957-963

Kwon, Y.D., Kwon, H.W., Kim, W. and Yeo, S.D. (2008), "Structural damage detection in continuum structures using successive zooming genetic algorithm", *Struct. Eng. Mech.*, **30**(2), 135-146

Law, S.S., Bu, J.Q., Zhu, X.Q. and Chan, S. L. (2006), "Vehicle condition surveillance on continuous bridges based on response sensitivity", *J. Eng. Mech.*, ASCE, **132**(1), 78-86

Li, H., Lu, Z.R. and Liu, J.K. (2016), "Structural damage identification based on residual force vector and response sensitivity analysis", *J. Vib. Control*, **22**(11), 2759-2770

Li, S. and Lu, Z.R. (2015), "Multi-swarm fruit fly optimization algorithm for structural damage identification", *Struct. Eng. Mech.*, **56**(3), 409-422

Lu, Z.R. and Law, S.S. (2007), "Features of dynamic response sensitivity and its application in damage detection", *J. Sound Vib.*, **303**(1-2), 305-329

Lu, Z.R. and Liu, J.K. (2011), "Identification of both structural damaged in bridge deck and vehicular parmeters using measured dynamic responses", *Comput. Struct.*, **89**, 1397-1405

Majumder, L. and Manohar, C.S. (2003), "A time domain approach for damage detection in beam structures using vibration data with a moving oscillator as an excitation source", *J. Sound Vib.*, **268**, 699-716

Mehrjoo, M., Khaji, N. and Mohsen, G.A. (2013), "Application of genetic algorithm in crack detection of beam-like structures using a new cracked Euler-Bernoulli beam element", *Appl. Soft Comput.*, **13**, 867-880

Miguel, F.F.L. and Lopez, R.H. (2013), "A hybrid approach for damage detection of structures under operational conditions", *J. Sound Vib.*, **332**, 4241-4260

Mohan, S.C., Maiti, D.K. and Maity, D. (2013), "Structure damage assessment using FRF employing particle swarm optimization", *Appl. Math. Comput.*, **219**, 10387-10400

Ratcliffe, C.P. (1997), "Damage detection using a modified Laplacian operator on mode shape data", *J. Sound Vib.*, **204**, 505-517

Sung, S.H., Koo, K.Y. and Jung, H.J. (2014), "Modal flexibility-based damage detection of cantilever beam-type structures using baseline modification", *J. Sound Vib.*, **333**, 4123-4138

Tab, Z., Afshri, E. and Morteza, H.B. (2013), "A new damage detection method: Big Bang-Big Cruch(BB-BC) algorithm", *Shock Vib.*, **20**, 633-648

Vakil-Baghmisheh, M.T., Peimani, M., Sadeghi, M.H. and Ettefagh, M.M. (2008), "Crack detection in Beam-like structures using genetic algorithms", *Appl. Soft Comput.*, **8**, 1150-1160

Xu, H.J., Ding, Z.H., Lu, Z.R. and Liu, J.K. (2015), "Structural damage detection based on Chaotic Artificial Bee Colony algorithm", *Struct. Eng. Mech.*, **55**(6), 1223-1235

Yang Q.W. (2011), "A new damage identification method based on structural flexibility disassembly", *J. Vib. Control*, **17**(7), 1000-1008

Yang, C. and Adams, D.E. (2014), "A damage identification technique based on embedded sensitivity analysis and optimization processes", *J. Sound Vib.*, **333**, 3109-3119

Yi, T.H., Zhou, G.D., Li, H.N. and Zhang, X.D. (2015), "Optimal sensor placement for health monitoring of high-rise structure based on collaborative-climb monkey algorithm", *Struct. Eng. Mech.*, **54**(2), 305-317

CC